V-I characteristics of X-ray conductivity and UV photoconductivity of ZnSe crystals

V. Ya. Degoda,[1,a)] M. Alizadeh,[1,b)] N. O. Kovalenko,[2] and N. Yu. Pavlova[3]
[1]*Taras Shevchenko National University of Kyiv, 64 Volodymyrs'ka Str., 01601 Kyiv, Ukraine*
[2]*Institute for Single Crystals NAS of Ukraine, Nauki Ave., Kharkiv 61001, Ukraine*
[3]*National Pedagogical Dragomanov University, Pyrogova Str., 9, 01601 Kyiv, Ukraine*

(Received 7 November 2017; accepted 28 January 2018; published online 20 February 2018)

This article outlines the resulting experimental V-I curves for high resistance ZnSe single crystals at temperatures of 8, 85, 295, and 420 K under three intensities of X-ray and UV excitations ($h\nu_{UV} > E_g$). This paper considers the major factors that affect the nonlinearity in the V-I curves of high resistance ZnSe. We observe superlinear dependences at low temperatures, shifting to sublinear at room temperature and above. However, at all temperatures, we have initial linear areas of V-I curves. Using the initial linear areas of these characteristics, we obtained the lifetime values of free electrons and their mobility. The comparison of the conductivity values of X-ray and UV excitations made it possible to reveal the fact that most of the electron-hole pairs recombine in the local generation area, creating a scintillation pulse, while not participating in the conductivity. When analyzing the nonlinearity of the V-I curve, two new processes were considered in the first approximation: an increase in the average thermal velocity of electrons under the action of the electric field and the selectivity of the velocity direction of the electron upon delocalization from the traps under the Poole-Frenkel effect. It is assumed that the observed nonlinearity is due to the photoinduced contact difference in potentials. *Published by AIP Publishing.* https://doi.org/10.1063/1.5012597

I. INTRODUCTION

Well-studied zinc selenide (ZnSe)[1–6] belongs to high-energy gap semiconductors $A^{II}B^{VI}$. For ZnSe crystals, the structure of the crystal lattice, the thermodynamic parameters, the width of the forbidden band, the effective masses of free electrons and holes and their mobility, the dielectric constant, and other parameters are known. Currently, ZnSe is widely used to create the devices of short-wave semiconductor electronics and information display systems.[7,8] This because in the last decade, people have learned to grow high-quality single crystals. Thus, another perspective area of ZnSe single crystal application appeared: using them as detectors of ionizing radiation with both indirect (gamma radiation scintillators)[9–13]and direct energy transformation of high-energy radiation into electric current (semiconductor detectors).[6,14–16] Besides, ZnSe is used widely for IR-area windows and lenses.[7,8,17,18] The use of the single crystal ZnSe as an ionizing radiation detector became possible after the proper development of crystal growing technology[19–21] with low concentrations of non-controllable admixtures and, hence, higher specific resistance of the material at $>10^{12}\,\Omega$ cm. A relatively high effective atomic number ($Z_{ef} = 32$) and a wide band of the forbidden zone (2.7 eV at 300 K) make ZnSe a prospective material for the creation of X-ray detectors which need no cooling and can function at temperatures substantially higher than room temperature (up to 450 K).[16] The design of a new semiconductor detector of ionizing radiation is impossible without detailed studies of its characteristics.

This fact actualizes the studies of X-ray conductivity (XRC) and X-ray luminescence (XRL) of ZnSe single crystals. The V-I curve of XRC is among principal characteristics of the semiconductor detectors of ionizing radiation. It was revealed earlier[22] that the V-I curve of XRC for ZnSe crystals is superlinear at room temperature. In general, the cases of Ohm law infringements for the semiconductors are known for a long time, and such processes are explained by the impact of admixture ionization, the Poole-Frenkel effect, Zener effect, the Gunn effect,[23,24] and the inhomogeneity of the sample.[25]

It was assumed in Ref. 22 that the nonlinearity of the V-I curve of XRC was due to the nature and features of the X-ray excitation. Therefore, the purpose of this work was an experimental research of the V-I curve under the X-ray and UV excitations of the ZnSe single crystals. These measurements should be done at different temperatures and at various intensities of X-ray and UV excitations. A comparison of the V-I curve for the two types of the excitations will help to explain the nonlinear dependences of the V-I curve. Considering that upon excitation triggering, we observe the buildup of both the luminescence and the conductivity, and then, at early research stages, it is logical to study the V-I curve for the equilibrium conditions of the crystal at constant temperatures.

II. EXPERIMENTAL PROCEDURE

We investigated the conductivity and luminescence of the ZnSe single crystals excited with X-ray and UV quanta. To obtain the crystals containing minimum impurity concentrations and having a maximum specific resistance ($\rho \geq 10^{12}\,\Omega$ cm), the undoped ZnSe crystals were grown from the purified charge.

a)degoda@univ.kiev.ua
b)trefoilsymbol@gmail.com

Also, the polished samples of $18 \times 9 \times 2\,mm^3$ were prepared. We should note that the concentrations of free electrons were $\sim 10^2\,cm^{-3}$ at room temperature and in the absence of excitation. It was preliminarily determined, by the thermal EMF method, that the samples have *n*-type dark conductivity (DC).

We carried out complex experimental research of X-ray conductivity (XRC), X-ray luminescence (XRL), photoluminescence (PL), photoconductivity (PC), and dark conductivity (DC). Upon excitation, we recorded phosphorescence and relaxation of the conductivity current, and then, we measured the thermally stimulated conductivity (TSC) and the thermally stimulated luminescence (TSL). To study the conductivity, the single crystals were sprayed by two three-layered metal contacts (sandwiches), using a resistive method. The contacts were fixed to one side in the center of the large sample side. The chemical composition of the sandwich was specially selected to provide (1) ohmic contacts for dark conductivity at 295 K, (2) with good adhesion of the contact and ZnSe, and (3) the ease of soldering wire to the contact. Earlier, it experimentally tested that the contact application and heating to 450 K did not change the luminescence characteristics of the samples. It was also found that the luminescence and conductivity of the samples were not changed for 4 years, when they were irradiated with X quanta, cooled to 8 K, and heated to 450 K. The contacts were the rectangular-shaped strips of $L = 5$ mm length and 1 mm width, and the distance between them was $d = 5$ mm. The copper conductors were soldered to electrical contacts to measure the conductivity. The stabilized voltage from 0 to 1000 V was applied to one of the electrodes, while the other was grounded through a nanoamperemeter. The following condition was met for all conductivity current values: the input impedance of the nanoamperemeter was a few orders lower than the electric resistance of the ZnSe sample. The nanoamperemeter was a component of the specially developed measuring unit, which allows selection of the voltage-measuring mode: manual, stepwise, and linear, which makes possible to change the voltage enhancement speed. The sample was placed in the cryostat, and the V-I curve was recorded at temperatures equal to 8, 85, 295, and 420 K. The selection of these temperatures is due to the absence of the need to use additional systems for stabilizing the temperature of the sample. The main thing is that these temperatures cover a wide temperature range. The studies of the V-I curve were conducted under vacuum conditions (<1 Pa).

The X-ray excitation was realized with integral radiation from a BXV X-ray tube (Re, 20 kV, currents running through the X-ray tube were 5, 15, and 25 mA) through a cryostat beryllium window in the direction perpendicular to the sample surface. The distance between the X-ray tube anode and the sample was 120 mm. When the current running through the X-ray tube changed and the voltage remained constant, the intensity of X-ray emission I_X changed proportionally, but the shape of the emission spectrum remained unchanged. As a result, the maximum intensity of X-ray irradiation of the sample (25 mA) was 0.635 mW/cm^2, at 15 mA, it was 0.38 mW/cm^2, and at 5 mA, the intensity was as large as 0.127 mW/cm^2.

For the band-to-band excitation, we used seven UV photodiodes of UF-301 type (wavelength at maximum irradiation of 395 nm, i.e., $h\nu_{UV} > E_g$) located in a single area $Ø = 20$ mm and equipped with a common power supply unit. The power supply unit of $7 \times$ LED allowed changing of the magnitude of the stabilized current within the 30 to 180 mA range. Each light-emitting diode (LED) irradiation was directed to the sample through the quartz window of a cryostat from the distance of 55 mm. Preliminarily, it was experimentally proven that the emission spectrum of light-emitting diodes (LEDs) does not depend on their power supply current. It allows us to change the intensity of the UV excitation by varying the magnitude of its current. The irradiation intensity (I_{UV}) of the sample was calibrated using an irradiation meter (IMO-2N measuring device of average power and energy of laser emanation). Three magnitudes of the intensity of UV excitation were used: 0.156 mW/cm^2 (180 mA), 0.075 mW/cm^2 (90 mA), and 0.030 mW/cm^2 (40 mA).

The conduction current and the luminescence radiation of the sample were recorded simultaneously allowing us to obtain more detailed and reliable information on the processes occurring in the sample. Two channels recorded the luminescence (at an angle of 45° to the normal): integrally and spectrally. The integral glow of the sample (if necessary through an optical filter) passed through the quartz window of the cryostat and then was focused with a quartz lens on the photocathode FEU-106. The luminescence radiation was passed via another quartz window of the cryostat through a high-speed monochromator MDR-2 with quartz condensers and was recorded using photoelectric multipliers: PMT-106 in the visible region or PMT-83 (in a cooling mode) in the IR region. All spectra were adjusted taking into account the spectral sensitivity of the recording system.

III. RESULTS OF THE EXPERIMENTAL RESEARCH

A. The XRL and PL spectra of high-resistance single crystal ZnSe samples in the spectral range of 400 to 1200 nm and at temperatures below 400 K consist of the two main luminescence bands with maxima at 630 nm (1.92 eV) and 970 nm (1.28 eV). For example, Fig. 1 shows the XRL spectra at two temperatures. The ratio of the intensities of these bands is different for various crystals. According to Refs. 20, 21, 26, and 27, the band having a maximum at 630 nm is caused by the complex center containing zinc vacancy. The band having a maximum at 970 nm is caused by complex center containing selenium vacancy or copper admixture.[28,29] The spectral positions of the bands' maxima and a ratio of the intensities do not change as excitement intensity changes. We should note that a dependence of the luminescence intensity of the external electric field is observed, as in Ref. 30. However, this intensity is very weak, and under low voltage conditions, the luminescence intensity remains within the measuring error. We should note as well that no boundary luminescence, as well as that of donor-acceptor pairs, was revealed within the XRL and PL spectra even at low temperatures and in the case of two-order raise in the sensitivity of the recording system.

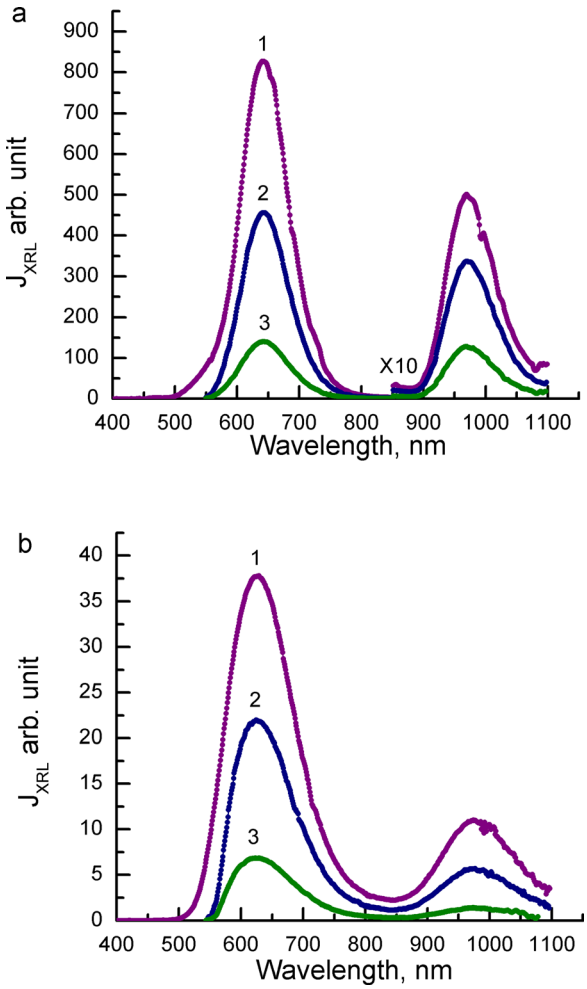

FIG. 1. The XRL spectra at *85 K (a) and 295 K (b) of the ZnSe crystal for ionizing intensities (current on the X-ray tube): 25 mA (0.635 mW/cm^2) (1), 15 mA (0.38 mW/cm^2) (2), and 5 mA (0.127 mW/cm^2) (3). *The intensity of dependence (970 nm) was multiplied by 10.

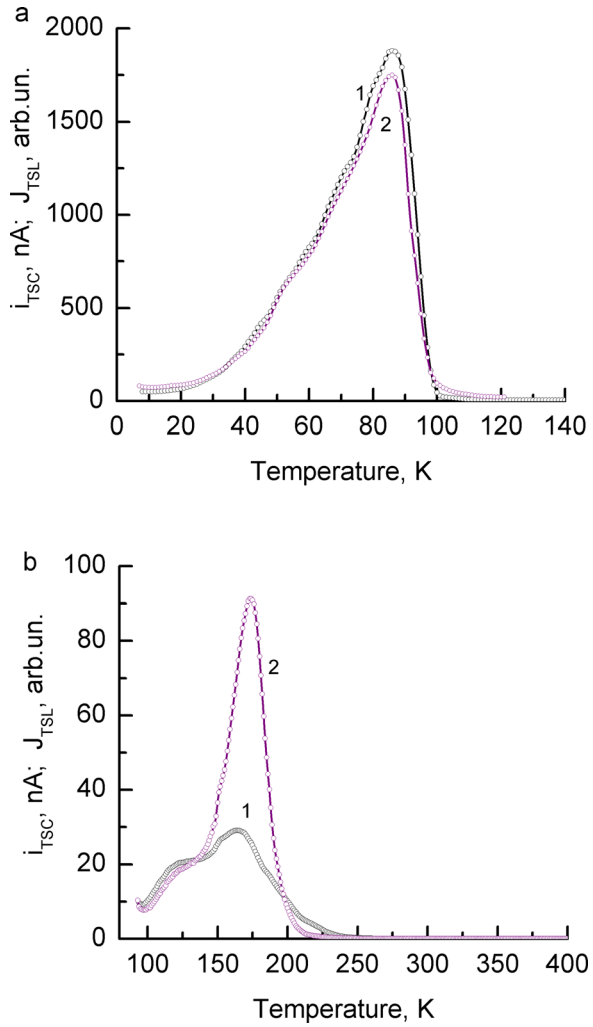

FIG. 2. Curves of TSC (1) (U = 15 V) and TSL (2) of the ZnSe sample after the 20 min period of its X-ray excitation at 8 (a) and 85 K (b).

The use of 4 temperatures (8, 85, 295, and 420 K) indicates that at these temperatures, generally, not only the mobility of free charge carriers (μ) but also their lifetime (τ) differs, which leads to different stationary concentrations of free electrons (N^-). The ratio between the concentrations of shallow and deep traps depends on the temperature. Therefore, first, it is necessary to be convinced about the presence of traps.

B. By using the methods of thermally stimulated luminescence (TSL) and conductivity (TSC), we recorded thermal delocalization of electrons from the traps upon excitation. Figure 2 shows the TSC and TSL curves for the ZnSe sample following the 20 min period of its X-ray excitation at 8 and 85 K. TSC and TSL peaks are clearly observed for the samples at up to 300 K temperature.

These peaks correlate well with the known traps in ZnSe crystals.[31] The same TSC and TSL peaks are observed at UV excitation, but their intensities are weaker. Therefore, at 8 K, all the traps within the crystal become deep, at 85 K, a portion of them becomes shallow, while deep ones are still available, and at 295 and 420 K, the number of deep traps decreases even more.

C. Dark conductivity of these samples is so low that it is hardly recorded at room temperature. One shall heat the sample above 370 K for its reliable recording. The temperature dependence of the dark conductivity is described well by the relationship of $i_D = Const \cdot \exp(-E/kT)$ with the energy of the electrons' thermal delocalization $E = 1.01$ eV. For ZnSe samples having lower resistance, the delocalization energy equals 0.83 eV and even 0.65 eV. These energy values coincide with possible energies of deep traps within ZnSe single crystals.[31]

D. X-ray conductivity and photoconductivity are a few orders higher than the dark conductivity. We should note that V-I curves are linear in the initial voltage range applied at all the temperatures and in various excitement modes. V-I curves derived experimentally at multiple temperatures and excitement intensities are shown in Figs. 3 and 4.

A similar comparison under the X-ray and UV excitations of luminescence and conductivity was studied for various crystals, including ZnO.[37–40]

We should note that at all the temperatures and excitation levels under both X-ray and UV excitations, all the V-I curves contain the initial linear part. It allows using the Ohm law for the determination of the conductivity parameters.

The experimental V-I curves are well approximated by the Poole-Frenkel curves at room temperature

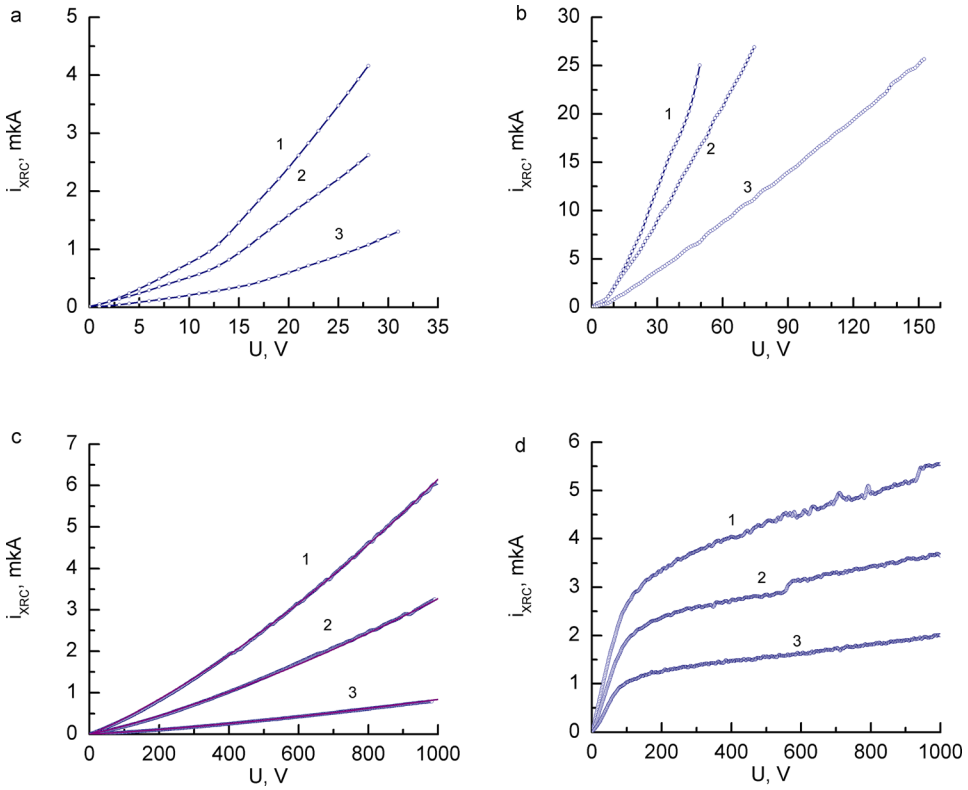

FIG. 3. V-I curve of the ZnSe sample at temperatures of 8 K (a), 85 K (b), 295 K (c), and 420 (d) at different X-excitation levels I_X: 0.635 mW/cm^2 (1), 0.38 mW/cm^2 (2), and 0.127 mW/cm^2 (3). The solid lines in (c) correspond to formula (1).

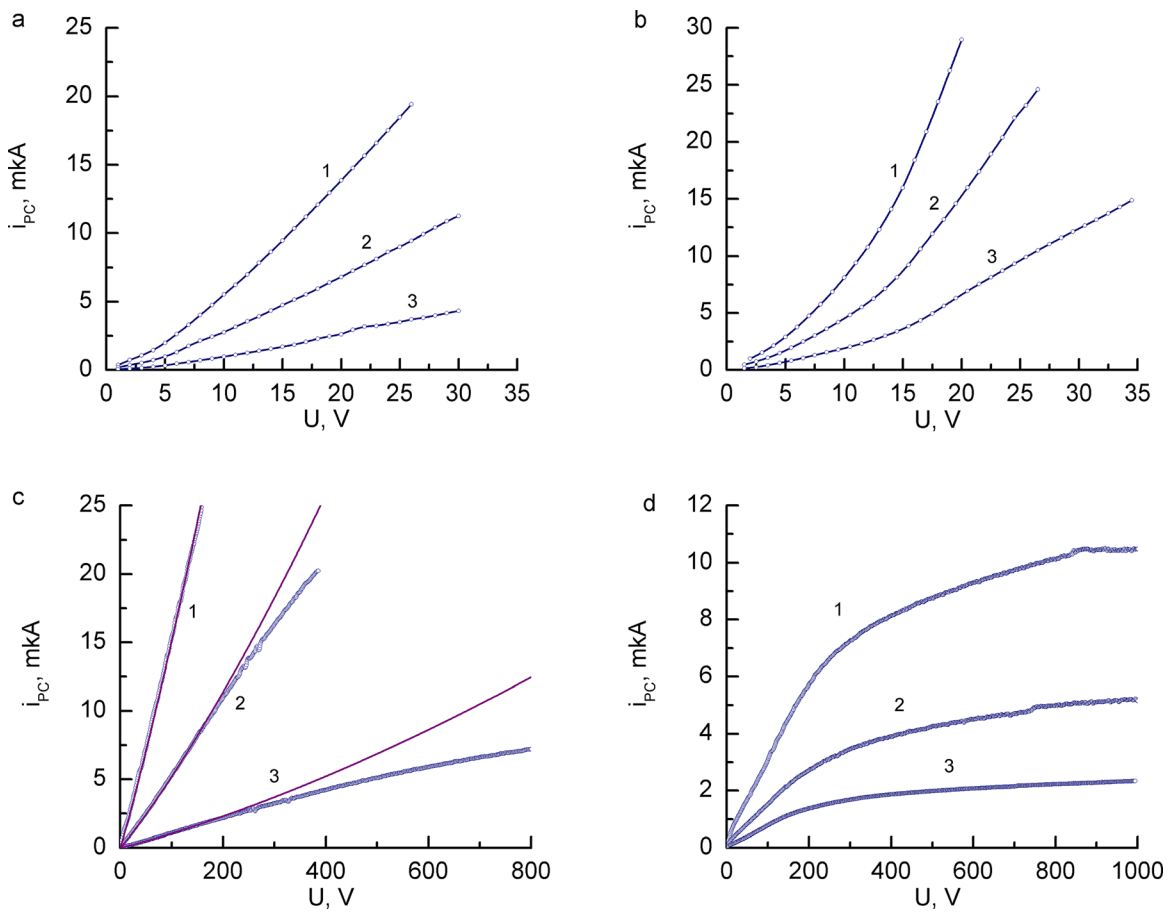

FIG. 4. V-I curve of the ZnSe sample at temperatures of 8 K (a), 85 K (b), 295 K (c), and 420 (d) at different levels of UV excitation I_{UV}: 0.156 mW/cm^2 (1), 0.075 mW/cm^2 (2), and 0.030 mW/cm^2 (3). The solid lines in (c) correspond to formula (1).

$$i_{XRC} = \frac{eI_X(1-C_{sc})L}{3E_g d}\mu^-\tau^- U\exp\left(\sqrt{C\,U}\right) \quad \text{and}$$
$$i_{PC} = \frac{eI_{UV}L}{h\nu_{UV}d}\mu^-\tau^- U\exp\left(\sqrt{C\,U}\right), \qquad (1)$$

where C constant is almost identical to the Poole-Frenkel constant ($C \approx e^3/2\pi\varepsilon\varepsilon_0 k^2T^2d$) and is identical to X-ray and UV excitation. These dependencies (1) are shown in Figs. 3(c) and 4(c) and approximate well the V-I curve of XRC and even PC at voltages up to 200 V. It means that it is necessary to consider in detail the Poole-Frenkel effect at excitation. At other temperatures being both higher and lower than room temperature, the dependencies (1) no longer fit for the V-I curve.

Generally, the experimentally derived V-I curve within the wide range of the voltages applied at various temperatures witnesses the infringement of the Ohm law for X-ray conductivity and photoconductivity of wide gap semiconductor ZnSe. Moreover, we observe clear superlinear V-I curve character. At above room temperature, the V-I curves change drastically: the curve transfer to the sublinear dependences.

IV. ANALYSIS OF THE EXPERIMENTAL RESULTS

The absorption of X-ray and UV quanta in the semiconductor leads to the generation of free electron-hole pairs, the number of which is proportional to the excitement intensity. By comparing V-I curves at X-ray and UV excitations at each temperature, we can see that they are very similar and have no principal difference.

First, we verified the similarity of V-I curves between each other at various intensity excitations. To do this, we plotted and analyzed the dependences of the current ratios for different excitement intensities (i_1/i_2, i_1/i_3, and i_2/i_3) on the voltage applied (the indices correspond to the numbers of the curves in Figs. 3 and 4). For all these dependencies, we observe a linear increase from the current with a small inclination, except for the initial area where the large dispersions of the experimental data are derived. The same phenomenon was observed in Ref. 22 under X-ray excitation. The experiment revealed that this feature of the V-I curve shape is observed in the case of UV excitation as well. One can assume that the insignificant differences in the shapes of the V-I curves are due to contact phenomena of the metal-ZnSe. It is sensible to assume that a contact potential difference, being dependent on the excitement intensity, will appear under intense permanent excitement when a high concentration of the charge carriers is generated. If this assumption is valid, the V-I curves should drift by the voltage scale at various excitement intensities. If we set some currents ratio $i_j(U+\Delta)/i_k(U)$, then it should be easy to choose the aΔ magnitude at which this current ratio has a constant value. In our case, this Δ magnitude ranges from 2 to 4 V for any ratios of the V-I curves at both XRC and PC. For example, Fig. 5 shows the corresponding ratios of the currents i_1/i_3 (curve 1) and $i_1(U+\Delta)/i_3(U)$ (curve 2) under X-ray excitation (85 K).

Thus, we can assume the appearance of a minor contact potential difference at the interface of the metal-ZnSe under X-ray and UV excitations, which explains some difference

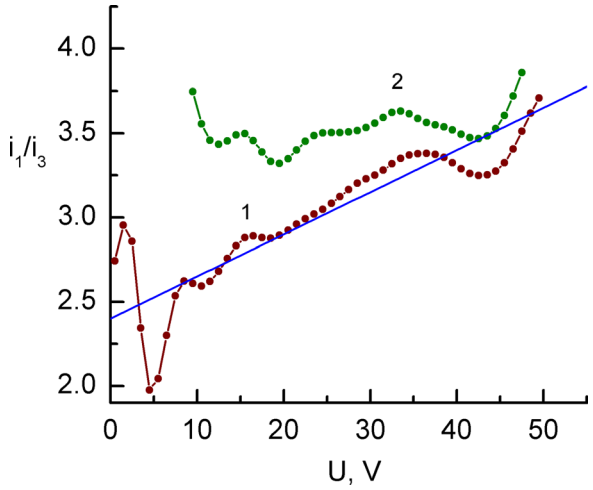

FIG. 5. The ratio of the XRC currents $i_1(U)/i_3(U)$ (1) and $i_1(U+\Delta)/i_3(U)$ (2) at $\Delta = 2$ V, 85 K.

in the shapes of the V-I curves. On the other hand, one shall conduct additional purposeful studies to derive well-defined evidence and define the values of the contact potential difference depending on the excitation intensity.

We shall proceed from the classical formula for the current density in semiconductors[23,24,33] from the field intensity (E) when considering the V-I curve in ZnSe. Bearing in mind the fact that the free holes have short lifetime compared to that of free electrons ($N^+ \ll N^-$)[1] and low mobility ($\mu^+ \ll \mu^-$),[1] they do not contribute significantly to XRC and PC

$$j = e\left(N^-\mu^- E + N^+\mu^+ E\right) \approx eN^-\mu^- E. \qquad (2)$$

During the experiment, the total current magnitude, not its density, is recorded. Therefore, the current's density magnitude needs to be integrated via the entire area of the generation of free charge carriers within the sample. The absorption of the radiation (I_X or I_{UV}) is described by the Beer–Lambert–Bouguer law and in the differential form appears as $dI(x) = I_0\cdot\kappa\cdot\exp(-\kappa x)\,dx$ under normal incidence on the sample, where I_0 is the intensity of the incident irradiation, κ = absorption coefficient of this irradiation, and x = depth within the sample. The special distribution of the generated charge carriers is to be determined by the following exponential relationship: $N^-(x) = N_0^-\cdot\exp(-\kappa x)$. Naturally, the relationship between I_0 and N_0^- will be different for X-ray and UV excitations. Bearing in mind that $dS = L\cdot dx$, for the selected record scheme of the conductivity current, we derive the following:

$$i = \int_S jdS = e\mu^- EL\cdot\int_0^\infty N^- dx$$
$$= e\mu^- EL\cdot\int_0^\infty N_0^-\exp(-\kappa x)dx = \frac{e\mu^- LU_0}{\kappa d}N_0^-. \qquad (3)$$

Under the absorption of X-ray quantum with $h\nu_x$ energy,[34,35] thousands of "hot" free electron-hole pairs are generated

$h\nu_x/(2.5 \div 3)E_g$ within a material having the width of the forbidden band (E_g), followed by a quick ($t < 10^{-11}$ s) thermalization of free charge carriers (free electrons and the hole lose the excess of their kinetic energy). The dimensions of the spatial domain of these electron and hole locations remain the same with a diameter of several microns. This is due to the Coulomb interaction between thousands of electrons with thousands of holes. Despite the fact that the difference in the effective masses of the electron and hole can reach 10 times, the spatial dimensions of an area containing these electrons and holes remain nearly unchanged and reach a few microns due to the coulomb interaction between thousands of electrons and thousands of holes. The presence of such a local excitation area is one of the specific features of X-ray excitation. A share of the generated electron-hole pairs recombines at the fluorescence centers in this local area, which creates a scintillation impulse. It is sensible to introduce a scintillation coefficient C_{sc} which determines a portion of the electron-hole pairs generated by the X-ray quantum, which creates a scintillation impulse. As a result, only a part ($1–C_{sc}$) of carriers will contribute to the X-ray conductivity and be localized at the traps. We can assume that under long X-ray excitation, a regular excitation takes place in the near-surface layer of $1/\kappa_x$ thick, but the $N^-(x)$ concentration is determined by the absorption coefficient (κ_x) of X-ray irradiation, its intensity (I_X), and free electron lifetime (τ^-) within the conductivity band: $N_0^- = \frac{I_X(1-C_{sc})\kappa_x\tau^-}{3E_g}$. In the case of ZnSe for $h\nu_x = 13$ keV (maximum of radiation at 20 kV), the absorption coefficient equals $\kappa_x \approx 250\,\text{cm}^{-1}$. It means that the depth of the excitation area is $1/\kappa_x \approx 40\,\mu$m, and X-ray conductivity current runs through this layer.

Under UV excitation in the semiconductor, the absorption of a single UV quantum leads to the transition of one electron from the valence zone to that of conductivity. One free electron-hole pair is generated, and a free electron and a hole have kinetic energy higher than the thermal (thermally equilibrium) velocity. However, the thermalization takes place for a period shorter than 10^{-11} s (due to the dispersal at point defects of the crystal structure and lattice phonons), while a free electron and a hole lose an excess of kinetic energy. The absorption of UV quanta takes place within some thin near-surface layer due to large absorption coefficients ($\kappa_{uv} > 10^4\,\text{cm}^{-1}$). This area widens to some extent due to diffuse thermal motion of free charge carriers, but the order of its magnitude remains $\sim 1\,\mu$m. Consequently, for the maximum concentration of free electrons, we derive the following: $N_0^- = \frac{I_{UV}\kappa_{UV}\tau^-}{h\nu_{UV}}$. Consequently, in the case of compliance with the Ohm law, we obtain the following simple equations for the X-ray and UV photoconductivity currents:

$$i_{XRC} = \frac{eI_X(1-C_{sc})L}{3E_g}\mu^-\tau^-E \text{ and } i_{PC} = \frac{eI_{UV}L}{h\nu_{UV}}\mu^-\tau^-E\,. \quad (4)$$

Thus, the nature of the exciting of the conductivity current is reduced to a general number of the generated electron-hole pairs.

All obtained V-I curves have the initial linear area which allows us to determine some parameters. Using the initial linear areas of the V-I curves ($di_{XRC}/dE \approx const$ and $di_{PC}/dE \approx const$), as well as appropriate intensities of X-ray and UV excitations, we can easily derive C_{sc} from Eq. (4) the following:

$$C_{sc} = 1 - \frac{di_{XRC}/dE}{di_{PC}/dE}\cdot\frac{I_{UV}}{h\nu_{UV}}\cdot\frac{3E_g}{I_X}. \quad (5)$$

The detained magnitudes are presented in Table I. We should note that these correlate well with the experimental dependences of the XRL intensity upon triggering the X-ray excitation. The availability of scintillations also explains the fact that the magnitudes of the XRC currents are much lower than those of the PC. As the intensity of the excitations (I_X and I_{UV}) and mobility of electrons within ZnSe at room temperature are known,[3] we can estimate a lifetime of a free electron. The obtained values equal to $\tau^-(\text{XRC}) = \tau^-(\text{PC}) = (3 \pm 1)\,\mu$s. We can state that the impurity concentration in high resistance ZnSe crystals is low since zero luminance of donor-acceptor pairs and zero boundary luminance are observed in the samples. It means that the mobility of free electrons within them, as in most $A^{II}B^{VI}$ crystals at $T > 100$ K, is determined by the dispersal at the lattice phonons and is consequently determined as follows:[23,24] $\mu \sim T^{-3/2}$. When the temperature increases above room temperature to 420 K, the electrons' mobility shall decrease 1.69 times and should be equal to 415 cm^2/V s. We can definitely derive a product of ($\mu^-\tau^-$) from the initial linear areas of the V-I curve. Exactly, this 1.7 times decrease was revealed. Therefore, we can suggest that the decrease in the conductivity at 420 K compared to that at room temperature is due to the decreased mobility of free electrons. A similar effect is to be observed at cooling. When the sample is cooled from 295 K to 85 K, the electrons' mobility shall increase by 6.46 times and reach 4500 cm^2/V s. A free electron lifetime[36] $\tau^- = (\sum u^-\sigma_d v_d)^{-1}$ is determined by its average thermal velocity (u^-), the concentrations of deep traps (v_d), and their sections for the electron localization (σ_d). Under such a temperature change, the concentration of deep traps increases, while a lifetime of a free electron can only decrease. Therefore, the experimentally derived increase in the product ($\mu^-\tau^-$) can be explained by increasing μ^-, whereas τ^- remains unchanged. A constant lifetime of electrons within a wide temperature interval witnesses the availability of a high concentration of extremely deep traps ($E_j > 1$ eV) in the sample. Obviously, the availability of such deep traps ensures the dark high resistance of these ZnSe samples at room temperature. When cooling the sample to 8 K, we observe an experimentally lowering of the product ($\mu^-\tau^-$). At such a low temperature, the scattering of free electrons at lattice phonons becomes insignificant in comparison to scattering at neutral and charged point defects, which is described

TABLE I. The values obtained for C_{sc}, μ and τ.

T, K	8	85	295	420
C_{sc}	0.88	0.80	0.90	0.50
μ, cm^2/V s	3450	4500	700	415
τ, μs	3	3	3	3

in Ref. 23 as follows: $\mu^- \sim T^{3/2}$. Under the excitation and at low temperature, the filling of all the traps and recharge of the luminescence centers occur. Naturally, at 8 K, the concentration of deep traps increases, while the localization section decreases.

As a result, the lifetime of the free electron will not change much compared to 85 K temperature. Therefore, it is logical to assume that a slight decrease of $\mu^-\tau^-$ is due to the decrease in electrons' mobility.

Thus, the magnitudes of the scintillation coefficients, the lifetime of a free electron, and its mobility were derived based on the linear areas of the V-I curve under X-ray and UV excitations.

The next significant question, which arose during the research of the V-I curve, is in the determination of the physical processes that cause a superlinear V-I curve in the wide temperature range. To our opinion, this cannot be an impact ionization of the impurity donors because such impurities are not observed in the samples under the spectroscopic studies and of the temperature dependences of the dark conductivity. Also, it cannot be caused by the increasing number of electrons within the conductivity band due to their transition from the valence band by the influence of the electric field (Zener effect). Moreover, it cannot be due to the increase in the delocalization probability from the local condition thanks to the electric field (the Poole-Frenkel effect in its classical form). Also, it cannot occur due to inhomogeneity in the samples.

A. Increase in the average electron's velocity in the electric field

The mobility of free electrons is determined by $\mu^- = \frac{e}{m^*}\frac{l^-}{u^-}$, where e is the their charge, m^* is the effective mass, l^- is the length of free run between the scattering acts, and u^- is the average thermal velocity. The ratio $\frac{l^-}{u^-} = \tau_t$ is conditionally called the duration of the electron free run. It is sensible to assume that the very magnitude of average velocity will change in the case of availability of the electric field and hence drift velocity. Therefore, we considered a model of the ideal gas which moves at constant velocity $u_0 (u_0 = \mu \mathrm{E})$. For the immovable laboratory system of coordinates, we obtained the following distribution of particles by their velocities:

$$f(u) = \frac{v}{u_0}\sqrt{\frac{m_0}{2\pi kT}} \cdot \left\{ \exp\left[-\frac{m_0(u-u_0)^2}{2kT}\right] - \exp\left[-\frac{m_0(u+u_0)^2}{2kT}\right] \right\}. \quad (6)$$

This distribution is different from the Maxwell distribution although the plots coincide at low values of u_0. The root-mean-square velocity was obtained as follows: $u_{\mathrm{rms}} = \sqrt{\frac{3kT}{m} + u_0^2} = \sqrt{\frac{3kT}{m}\left(1 + \frac{m u_0^2}{3kT}\right)}$, but a simple expression in an analytical form for the average velocity is not derived. For the Maxwell distribution, the ratios between the most probable velocity, average velocity, and root-mean-square velocity (u_{rms}) remain constant and do not depend on the particles' mass and temperature. Taking into account that the derived distribution (6) does not significantly differ from the Maxwell distribution, we can make use of this and put down as follows for the average velocity: $u^- = u_{rms}\sqrt{\frac{8}{3\pi}} = \sqrt{\frac{8kT}{\pi m}\left(1 + \frac{m u_0^2}{3kT}\right)}$. Thus, the appearance of a constantly drifting velocity leads to $\sqrt{1 + \frac{m u_0^2}{3kT}}$ times rising of the average velocity of the particles.

The X-ray and UV excitations lead to the appearance of a high average concentration of free charge carriers within the excitation area. In addition, they allow us to apply the statistical physics laws and, in particular, to use the ideal gas model for the free electrons. The increase in the average velocity of the free electron motion indicates an increase in mobility by the same number of times: $\mu = \mu_0\sqrt{1 + \frac{m* u_0^2}{3kT}}$. By substituting the value of the constant velocity ($u_0 = \mu \mathrm{E}$) in this equation and then solving it, with respect to $\mu(\mathrm{E})$, we get $\mu = \frac{\mu_0}{\sqrt{1 - \frac{m*(\mu_0^- E)^2}{3kT}}}$. As a result, the dependence of current on voltage takes the following form:

$$i_{XRC} = \frac{eI_X(1-C_{sc})L}{3E_g}\frac{\mu_0^-\tau^- E}{\sqrt{1 - \frac{m^*(\mu_0^- E)^2}{3kT}}} \quad \text{and}$$
$$i_{PC} = \frac{eI_{UV}L}{h\nu_{UV}}\frac{\mu_0^-\tau^- E}{\sqrt{1 - \frac{m^*(\mu_0^- E)^2}{3kT}}}. \quad (7)$$

This dependence is nonlinear. It is obvious that noticeable nonlinearity will be observed when the drift velocity value approaches to the magnitude of the average thermal velocity of a free charge carrier. Because at low temperature, the average thermal velocity will be minimal, while the mobility close to maximal, the V-I curve nonlinearity must be observed most clearly at 8 K.

A comparison of the dependence for the current (7) with the experimental results [Figs. 3(a) and 4(a)] shows that this relation does not provide sufficient superlinearity for the V-I curve. Using $m^* = 0.17 \cdot m_e$ and μ_0 from Table I, we find out that the coefficient $(m^* \mu_0^2/3kT)$ is 3 to 4 orders smaller than that required for the description of the experimentally observed superlinearity of the V-I curve. Let us note that for all obtained experimental results, the following condition was satisfied: the drift velocity remained much lower for the average thermal velocity of the free electron.

The superlinear rise in the V-I curve of XRC and PC at 8 K cannot be explained by impact ionization of electrons as well even from a shallow trap [$E_T = 0.038$ eV (Ref. 31)] because both the electron's thermal energy and the energy secured by an electron from the electric field between the two consequent scattering acts remain much lower than the trap depth.

B. The influence of the Poole-Frenkel effect on UV photoconductivity

The Poole-Frenkel effect in its classic form shows an increase in the probability of the charge carrier delocalization

from the local level of point defects of depth E_T, which leads to the increase in the concentration of the free carriers and decrease in the concentration of the localized ones. This phenomenon is significant for the dark conductivity,[32] but in the case of X-ray or UV excitation, such a large number of electron-hole pairs are generated, which largely exceeds dark concentrations of free charge carriers. Therefore, the delocalization probability increase itself will not significantly influence the XRC and PC of a semiconductor. According to quantum-mechanical concepts of the solid-state physics, the spatial change in the point defect potential will take place in the case of electric field availability.[23,24] The Poole-Frenkel effect itself is based on the assumption of the coulomb potential for a point localization center. Usually, the maximum potential decrease for a localized charge carrier is commonly considered within a field (E) in a semiconductor having a dielectric constant equal to ε[32]

$$\Delta E_{PF} = \sqrt{\frac{e^3 E}{\pi\varepsilon\varepsilon_0}}. \tag{8}$$

The potential barrier for the delocalization is of minimum magnitude along the direction of the drift velocity of free electrons, but it rises in the opposite direction. The initial direction of motion of a delocalized electron is equiprobable for all directions in the case of the absence of the external field ($\boldsymbol{E} = 0$). If the carrier's velocity at localization on a trap is equal to its average thermal velocity, the initial velocity at delocalization has to be equal to an average thermal value (u) according to the law of energy preservation. We omit the "–" superscript because we do not consider the processes of the electron localization and delocalization in this study. In the case of the presence of the external field ($\boldsymbol{E} \neq 0$), the initial velocities of the delocalized carriers shall also be equal to the average thermal velocity, but the initial directions shall no longer be of equal probability. It means that the large portion of the delocalized electrons will have the initial velocity directed along the drift velocity. As a result of this symmetry of the initial velocity directions, we can assume that all delocalized electrons shall have an additional velocity (u_{PF}). We can introduce φ being the angle between the direction of the drift velocity and the initial direction of motion of a delocalized carrier. The magnitude of the field along the direction of φ equals $\boldsymbol{E}$ Cos φ, and hence, the barrier magnitude will decrease by $\Delta E_{PF} = \sqrt{\frac{e^3 E\cos\varphi}{\pi\varepsilon\varepsilon_0}} \approx \sqrt{\frac{e^3 E}{\pi\varepsilon\varepsilon_0}}\cos\varphi$. The substitution of $\sqrt{\cos\varphi}$ by $\cos\varphi$ was made to simplify the calculations and did not influence principally the physical result. First, these functions do not differ significantly, and secondly, by doing this, we decrease the probability of the delocalization along the φ direction. It is obvious that the probability of delocalization $\varphi = \pi/2$ does not change. In fact, we simplify the model a bit by using the relationship of $\Delta E_{\mathrm{PF}}{\cdot}Cos\varphi$ to change the barrier height. For such a model of center, we derive the raising probability of the delocalization in the φ direction $\left(w_0 \exp\left[-\frac{E}{kT} + \frac{\Delta E_{PF}}{kT}\cos\varphi\right]\right)$, which leads to the decrease in the delocalization along the opposite direction ($\varphi + \pi$).

Let us sum up all the projections of the velocities of the delocalized electrons against the direction of the drift velocity and divide by the total number of the delocalization acts for the Δt period in order to determine u_{PF} as follows:

$$\begin{aligned} u_{PF} &= \frac{\int_0^{2\pi} n_s \Delta t\, u\cos\varphi\, w_0 \exp\left(-\frac{E_s}{kT} + \frac{\Delta E_{PF}}{kT}\cos\varphi\right) d\varphi}{\int_0^{2\pi} n_s \Delta t\, w_0 \exp\left(-\frac{E_s}{kT} + \frac{\Delta E_{PF}}{kT}\cos\varphi\right) d\varphi} \\ &= \frac{2n_s \Delta t w_0 \exp\left(-\frac{E_s}{kT}\right)\int_0^{\pi} u\cos\varphi\, w_0 \exp\left(\frac{\Delta E_{PF}}{kT}\cos\varphi\right) d\varphi}{2n_s \Delta t\, w_0 \exp\left(-\frac{E_s}{kT}\right)\int_0^{2\pi} \exp\left(\frac{\Delta E_{PF}}{kT}\cos\varphi\right) d\varphi} \\ &= \frac{\int_0^{\pi} u\cos\varphi\, w_0 \exp\left(\frac{\Delta E_{PF}}{kT}\cos\varphi\right) d\varphi}{\int_0^{2\pi} \exp\left(\frac{\Delta E_{PF}}{kT}\cos\varphi\right) d\varphi} \\ &\cong u\left[1 - \exp\left(-\frac{\Delta E_{PF}}{2kT}\right)\right], \end{aligned} \tag{9}$$

where n_s is a concentration of the localized electrons at s-type traps of depth E_s and a frequency factor w_0. The obtained equation cannot be integrated in the elementary functions. It is obvious from the physical viewpoint that in the case of an increase in the field, u_{PF} shall approach asymptotically to the average thermal velocity of u. Therefore, we selected the approximated simple analytical function to describe u_{PF}.

Such an approach is legitimate as we calculate the added velocity within the proposed model.

Thus, in the case of an external field, due to the asymmetry of the directions of the electron delocalization from the trap, we derive that the delocalized carriers have additional initial velocity u_{PF} directed in parallel to the drift velocity, while its magnitude is determined by that of the field and does not depend on the trap depth.

This phenomenon for XRC and PC will appear under electrons' delocalization at all the traps, but the greatest efficiency will take place at shallow ones, and as per time unit, the major number of delocalization acts will happen at the shallow traps.

Let us determine the number of the electron delocalization acts from shallow traps per time unit. Under the equilibrium condition, the number of delocalization acts from any traps per time unit equals the number of the electron delocalization acts from them. For shallow traps, this balance is as follows:

$$N^- u\,\sigma_s v_s = n_s w_0 \exp\left(-\frac{E_s}{kT}\right)\exp\left(\frac{\Delta E_{PF}}{kT}\right). \tag{10}$$

It is more convenient to use a number of delocalization acts for the calculations, as they contain only a single variable, i.e., the concentration of free electrons, which determines the magnitude of conductivity current. If we take into account that the average lifetime of a free electron $\tau = (u\sigma_d v_d)^{-1}$ is determined by the concentration of deep traps (v_d), then $u\,\sigma_s v_s \tau^- = \frac{\sigma_s v_s}{\sigma_d v_d}$ Thus, each free electron contributing to the conductivity gets additional velocity u_{PF} ($\sigma_s v_s/\sigma_d v_d$). However, any delocalized electron will have the extra velocity only until the first scattering act (τ_t), or at a crystal lattice defect or at a lattice phonon. The ratio $\left(\frac{\sigma_s v_s}{\sigma_d v_d}\right)$ determines an average number of acts of intermediate electron localization at shallow traps for the electron lifetime in its free state. As a result, the ratio $\left(\frac{\sigma_s v_s}{\sigma_d v_d} \cdot \frac{\tau_t}{\tau^-}\right)$ shows what part of time the electron has the additional velocity Δu_{PF}. The work of this ratio by the additional velocity u_{PF} gives a time-averaged additional velocity for all electrons, directed parallel to the drift velocity:

$$\begin{aligned}\Delta u_{PF} &= \frac{\sigma_s v_s}{\sigma_d v_d}\frac{\tau_t}{\tau^-}u_{PF} \\ &= \frac{\mu m^* u^2}{e}\frac{\sigma_s v_s \cdot \sigma_d v_d}{\sigma_d v_d}\left[1 - \exp\left(-\frac{\Delta E_{PF}}{2kT}\right)\right] \\ &= \frac{3\mu kT\,\sigma_s v_s}{e}\left[1 - \exp\left(-\frac{\Delta E_{PF}}{2kT}\right)\right]. \end{aligned} \tag{11}$$

Thus, the total drift velocity is to be determined as follows bearing in mind the Poole-Frenkel effect:

$$\begin{aligned} u_{dr} &= \mu E + \Delta u_{PF} \\ &= \mu\left\{E + \frac{3\,kT\,\sigma_s v_s}{e}\left[1 - \exp\left(-\frac{\Delta E_{PF}}{2kT}\right)\right]\right\}. \end{aligned} \tag{12}$$

Hence, at the semiconductor excitement, we derive the following for the V-I curve:

$$\begin{aligned} i_{XRC} &= \frac{eI_X(1-C_{sc})L}{3E_g}\mu^-\tau^- \\ &\quad\times\left\{E + \frac{3\,kT\,\sigma_s v_s}{e}\left[1 - \exp\left(-\sqrt{\frac{e^3E}{4\pi\varepsilon\varepsilon_0 k^2T^2}}\right)\right]\right\} \text{ and} \\ i_{PC} &= \frac{eI_{UV}L}{h\nu_{UV}}\mu^-\tau^- \\ &\quad\times\left\{E + \frac{3\,kT\,\sigma_s v_s}{e}\left[1 - \exp\left(-\sqrt{\frac{e^3E}{4\pi\varepsilon\varepsilon_0 k^2T^2}}\right)\right]\right\}. \end{aligned} \tag{13}$$

The dependence $\left\{\frac{3\,kT\,\sigma_s v_s}{e}\left[1 - \exp\left(-\sqrt{\frac{e^3E}{4\pi\varepsilon\varepsilon_0 k^2T^2}}\right)\right]\right\}$ at low electric field intensities is proportional to ΔE_{PF}, which further transfers to the sublinear dependence. It should be noted that the dependencies (13) are functionally very similar to the V-I curve, which gives the Poole-Frenkel effect. Second, this conductivity add-on will be quite insignificant in the case of high-quality semiconductor materials ($v_s < 10^{15}\,\text{cm}^{-3}$).

The experimental studies of the dark conductivity in ZnSe crystals[32] confirm the influence of the Poole-Frenkel effect on the V-I curve. In the case of equilibrium stationary excited crystal conditions, the filling of each *i*-th type trap is described by the following equation:[36]

$$N^- u^-\,\sigma_i(v_i - n_i) - n_i w_{0i}\exp\left(-\frac{E_{Ti}}{kT}\right) - N^+ u^+ \sigma_r^+ n_i = 0. \tag{14}$$

The first summand in this equation determines the trap filling with free electrons, whereas the second one determines thermal delocalization from the trap, and the third summand stands for the recombination (usually without any emanation) of free holes with localized electrons. Depending on the trap depth (E_i) and temperature, different summands will dominate in this equation, and hence, various levels of filling of this trap (n_i/v_i) will take place. The probability of electron delocalization from deep traps is very low, and even its enhancement due to the Poole-Frenkel effect will not influence both the extent of their filling and concentration of free electrons within the conductivity band. The luminescence intensity is determined by the product of the concentration of free electrons and the concentration of the recharged fluorescence centers and remains constant with accurately 7% in the case of X-ray excitation and 2% in the case of UV excitation under the availability of an electric field, according to the experimental results. At that, the magnitudes of the XRC and PC currents grow by tens of percent or even a number of times compared to the linear dependence of the V-I curve. It means that the concentration of the free electrons remains unchanged under the increasing field. Another confirmation of this phenomenon is the initial magnitude of the relaxation of the conductivity current and phosphorescence. Experimentally, in all cases, we observe a decrease (at least by 1.5 to 2 orders) in the conductivity current magnitude and luminescence intensity when excitation is turned off.

In the case of shallow traps, the localization probability is very high, which leads to low filling levels of these traps; at that, Eq. (14) transfers to Eq. (10). The Poole-Frenkel effect also increases the delocalization probability and reduces the average duration of the presence of the electron in a localized state. Bearing in mind the relationships of the localization section (σ_s) and frequency factor (w_{0s}),[33] we can determine a concentration of the localized electrons at a shallow s-type trap using a concentration of free electrons within the conductivity band and $N_C = 2\left(\frac{2\pi m_e kT}{h^2}\right)^{\frac{3}{2}}$ being an effective density of the electrons' state in the conductivity band as follows:

$$n_s = N^-\frac{\nu_s}{N_C}\exp\left(\frac{E_s}{kT}\right)\exp\left(-\frac{\Delta E_{PF}}{kT}\right). \tag{15}$$

Thus, the Poole-Frenkel effect changes a level of filling of shallow traps but not the concentration of free electrons. A careful consideration of the influence of the Poole-Frenkel effect on the photo- and X-ray conductivities shows that this process does not cause the nonlinearity of the V-I curve. The concentrations of shallow traps will be the highest in semiconductors at high temperatures.

Thus, generally, the nonlinear character of the V-I curves in the case of X-ray or UV excitation is due to some principally new and unknown process or is caused by metal-ZnSe near-contact phenomena. The generation of a great number of free charge carriers within a semiconductor creates an additional non-uniform electric field within the near-contact area. We assume that no other known effects can explain the V-I curves observed in practice under X-ray and UV excitations.

V. CONCLUSIONS

The comparison of X-ray conductivity with UV photoconductivity within ZnSe crystals showed that the principal difference lies in the fact that under X-ray irradiation, the considerable portion of the electron-hole pairs does not contribute to the conductivity but recombines within the local generation area which creates a scintillation impulse. The general character of the V-I curve does not depend on the excitation at temperatures between 8 and 420 K. All V-I curves at low temperatures are superlinear, but at temperatures higher than room temperature, they transfer to the sublinear ones. In analyzing the nonlinearities of the V-I curves, in the first approximation, two new processes were considered: an increase in the average thermal velocity of electrons under the action of an electric field and the selectivity of the electron velocity direction during delocalization from the traps in the framework of the Poole-Frenkel effect. Evidently, the experimentally observed nonlinearity of the V-I curve is caused by the photoinduced contact potential difference under X-ray and UV excitations of ZnSe crystals.

[1]*Physics of A2B6 Compounds*, edited by A. N. Georgobiani and M. K. Sheinkman (Nauka, Moscow, 1986) (in Russian).
[2]D. D. Nedeoglo and A. V. Simashkevich, *Electrical and Luminescence Properties of Zinc Selenide* (Shtiintsa, Kishinev, 1984) (in Russian).
[3]V. I. Gavrilenko, A. M. Grekhov, D. V. Korbutyak, and V. G. Litovchenko, *Optical Properties of Semiconductors: A Handbook* (Naukova Dumka, Kiev, 1987) (in Russian).
[4]N. K. Morozova, V. A. Kuznetsov, V. D. Ryzhikov, V. G. Galstyan, and D. V. Kostomarov, *Zinc Selenide: Production and Optical Properties* (Nauka, Moscow, 1992) (in Russian).
[5]G. A. Bordovsky, "X-ray conductivity of high-resistance semiconductors," Soros Educ. J. **7**(3), 84–89 (2001).
[6]V. Y. Degoda and A. O. Sofiienko, "Specific features of the luminescence and conductivity of Zinc Selenide on exposure to X-ray and optical excitation," Semiconductors **44**(5), 568–574 (2010).
[7]L. V. Atroshchenko, S. F. Burachas, L. P. Galchinetski, B. V. Grinev, V. D. Ryzhikov, and N. G. Starzhinskii, *Scintillation Crystals and Ionization Radiation Detectors on Their Base* (Naukovadumka, Kiev, 1998) (in Ukrainian).
[8]V. D. Ryzhikov, *Scintillation Crystals of Semiconductor Compounds AIIBVI* (NIITEHIM, Moscow, 1989) (in Russian).
[9]I. Dafinei, M. Fasoli, F. Ferroni, E. Mihokova, F. Orio, S. Pirro, and A. Vedda, "Low temperature scintillation in ZnSe crystals," IEEE Trans. Nucl. Sci. **57**(3), 1470–1474 (2010). [5485159].
[10]N. Starzhinkiy, B. Grinyov, I. Zenya, V. Ryzhikov, L. Gal'chinetskii, and V. Silin, "New trends in the development of AIIBVI-based scintillators," IEEE Trans. Nucl. Sci. **55**, 1542–1546 (2008).
[11]V. D. Ryzhikov *et al.*, "Properties of semiconductor scintillators ZnSe(Te,O) and integrated scintielectronic radiation detectors based thereon," IEEE Trans. Nucl. Sci. **48**(1), 356–359 (2001).
[12]Y. H. Cho, S. H. Park, W. G. Lee, J. H. Ha, H. S. Kim, N. Starzinskiy, D. H. Lee, S. Park, and Y. K. Kim, "Comparative study of a CsI and a ZnSe(Te/O) scintillation detector's properties for a gamma-ray measurement," J. Nucl. Sci. Technol. **45**(5), 534–537 (2008).
[13]V. Ryzhikova, G. Tamulaitisb, N. Starzhinskiya, L. Gal'chinetskiia, A. Novickovasb, and K. Kazlauskas, "Luminescence dynamics in ZnSeTe scintillators," J. Lumin. **101**, 45–53 (2003).
[14]A. O. Sofiienko and V. Y. Degoda, "X-ray induced conductivity of ZnSe sensors at high temperatures," Radiat. Meas. **47**, 27 (2012).
[15]M. S. Brodin, V. Y. Degoda, B. V. Kozhushko, and A. O. Sofíênko, Sens. Electron. Microsyst. Technol. **2**(8), 25 (2011) (in Russian).
[16]M. S. Brodin, V. Y. Degoda, B. V. Kozhushko, A. O. Sofiienko, and V. T. Vesna, "Monocrystalline ZnSe as an ionising radiation detector operated over a wide temperature range," Radiat. Meas. **65**, 36–44 (2014).
[17]D. B. Elmurotova and E. M. Ibragimova, "Amplification of electroluminescence of ZnSe (Te, O) crystals after γ-irradiation," Phys. Technol. Semicond. **41**(10), 1153–1157 (2007).
[18]A. Nasr, A. Aboshosha, and M. Ashour, "Performance evaluation of phototransistors and their behavior under gamma radiation effects," in EG0800227, The Second All African IRPA Regional Radiation Protection Congress, Ismailia Egypt (2007).
[19]E. Krause *et al.*, "Influence of growth non-stoichiometry on optical properties of doped and non-doped ZnSe grown by chemical vapour deposition," J. Cryst. Growth **138**, 75–80 (1994).
[20]V. M. Koshkin, A. Y. Dulfan, and V. D. Ryzhikovetal, "Thermodynamics of isovalent tellurium substitution for selenium in ZnSe semiconductors," J. Funct. Mater. **8**(N4), 708–713 (2001).
[21]G. Watkins, "Defects of lattice in compounds A2B6," in *Point Defects of Lattice* (Mir, Moscow, 1979), pp. 221–242.
[22]V. Y. Degoda and G. P. Podust, "X-ray conductivity of ZnSe single crystals," Semiconductors **50**(5), 579–585 (2016).
[23]P. S. Kireev, *Physics of Semiconductors* (Higher School, Moscow, 1975).
[24]K. V. Shalimova, *Physics of Semiconductors* (Énergiya, Moscow, 1971).
[25]U. Philipose, H. E. Ruda, A. Shik, C. F. de Souza, and P. Sun, "Conductivity and photoconductivity in undoped ZnSe nanowire array," J. Appl. Phys. **99**, 66106 (2006).
[26]V. D. Ryzhikov, N. G. Starzhinskiy, L. P. Gal'chinetskii *et al.*, Int. J. Inorg. Mater. **3**, 1227–1229 (2001).
[27]L. Huan-Yong, J. Wan-Qi, Z. Shi-An, S. Zhen-Rong, and X. Ke-Wei, "The photoluminescence of ZnSe bulk single crystals excited by femtosecond pulse," Chin. Phys. **15**(10), 2407–2408 (2006).
[28]F. J. Bryant and P. S. Manning, J. Phys. C **5**, 1914–1920 (1972).
[29]N. K. Morozova, I. A. Karetnikov, V. V. Blinov, and E. M. Gavrishchuk, Semiconductors **35**, 512–515 (2001).
[30]V. Ya. Degoda and A. O. Sofienko, "Specific features of the luminescence and conductivity of zinc selenide on exposure to X-ray and optical excitation," Semiconductors **44**(5), 594–599 (2010).
[31]V. Degoda, A. Gumenjuk, N. Pavlova, A. Sofiienko, and S. Sulima, "Oscillatory regularity of charge carrier trap energy spectra in ZnSe single crystal," Acta Phys. Pol. **129**(3), 304–309 (2016).
[32]V. Y. Degoda and G. P. Podust, "Features of the dark conductivity of zinc selenide," Semiconductors **48**(3), 273–280 (2014).
[33]R. H. Bube, *Photoconductivity of Solids* (John Wiley & Sons, New York, 1960).
[34]A. M. Gurvich, *X-ray Fluorescence and X-ray Screens* (Atomizdat, Moscow, 1976).
[35]V. Y. Degoda and A. O. Sofiienko, "Spatial generation of electronic excitations at the absorption of X-rays," Ukr. J. Phys. **52**(3), 256–264 (2007) (in Ukrainian).
[36]V. Y. Degoda, A. F. Gumenjuk, and Y. A. Marazuev, *The Kinetic of Recombination Luminescence and Conductivity of Crystalophosphors* (Taras Shevchenko National University of Kyiv VPT, The University of Kyiv, 2016).
[37]J. Ji, A. M. Colosimo, W. Anwand, L. A. Boatner, A. Wagner, P. S. Stepanov, T. T. Trinh, M. O. Liedke, R. Krause-Rehberg, T. E. Cowan, and F. A. Slim, "ZnO luminescence and scintillation studied via photoexcitation, X-ray excitation, and gamma-induced positron spectroscopy," Sci. Rep. **6**, 31238 (2016).
[38]A. Janotti and C. G. Van de Walla, "Fundamentals of zinc oxide as a semiconductor," Rep. Prog. Phys. **72**(12), 126501 (2009).
[39]C. R. Varney, M. A. Khamehchi, J. Ji, and F. A. Selim, "X-ray luminescence based spectrometer for investigation of scintillation properties," Rev. Sci. Instrum. **83**, 103112 (2012).
[40]F. A. Selim, M. H. Weber, D. Solodovnikov, and K. G. Lynn, "Nature of native defects in ZnO," Phys. Rev. Lett. **99**, 085502 (2007).